Spatio-temporal investigation of the crosslinking and the mechanical properties in a UV-curable rubber bearing photo-dimerizable moieties

S Colanges, K Ballu, A Lamouroux, Gilles Pecastaings, Isabelle Ly, Cédric Le Coz, Thierry Tassaing, T Brunet, Etienne Grau, Henri Cramail, et al.

Spatio-temporal investigation of the crosslinking and the mechanical properties in a UV-curable rubber bearing photo-dimerizable moieties

Colanges, S.;[1, 2, 3] Ballu, K.;[1, 2, 3] Lamouroux, A.;[1, 2, 3] Pecastaings, G.;[2] Ly, I.;[2] Le Coz, C.;[1] Tassaing, T.;[4] Brunet, T.;[3] Grau, E.;[1] Cramail, H.; [1] Mondain-Monval, O.; [2,*] Vidil, T.[1,*]

[1] University of Bordeaux – CNRS – Bordeaux INP, LCPO, 16 avenue Pey-Berland 33600 Pessac, France

[2] University of Bordeaux – CNRS – Centre de Recherche Paul Pascal, Pessac, France

[3] University of Bordeaux – CNRS – Bordeaux INP, Institut de Mécanique et d'Ingénierie, Talence, France

[4] University of Bordeaux – CNRS – Bordeaux INP, Institut des Sciences Moléculaires, Talence, France

Abstract

A polybutadiene rubber was functionalized with UV-dimerizable cinnamic moieties using thiol-ene click chemistry and the resulting polymer was used to prepare millimeter-thick objects with photo-tunable modulus. The crosslink density was modulated by controlling the irradiation time t under UV. For this purpose, the kinetics of the photo-crosslinking reaction was first investigated *via* conventional photo-rheology and infrared spectroscopy analyses. In parallel, Raman spectroscopy was used to probe the evolution of the crosslink density as a function of depth from the irradiated surface. These measurements provide insights into the crosslink density's evolution, both over time and as a function of depth within the samples. They reveal gradient profiles with diminishing amplitude over longer irradiation times. After 4 hours of irradiation, the crosslink density becomes mostly homogeneous. The concurrent investigation of the mechanical properties indicates that the elastic modulus of the materials can be varied over almost three orders of magnitude (4 MPa $\leq E \leq$ 2 GPa), by varying the exposure time within a relatively small window (5 min $\leq t \leq$ 240 min). To challenge the data collected in Raman spectroscopy, Atomic Force Microscopy nanoindentation was used for the local investigation of the modulus, within the materials. The results confirmed the presence of modulus gradients consistent with those of the crosslink density. This unprecedented study of the spatio-temporal evolution of crosslink density in a UV-crosslinkable polymer offers valuable insights for applications requiring soft materials with photo-tunable mechanical properties.

TOC

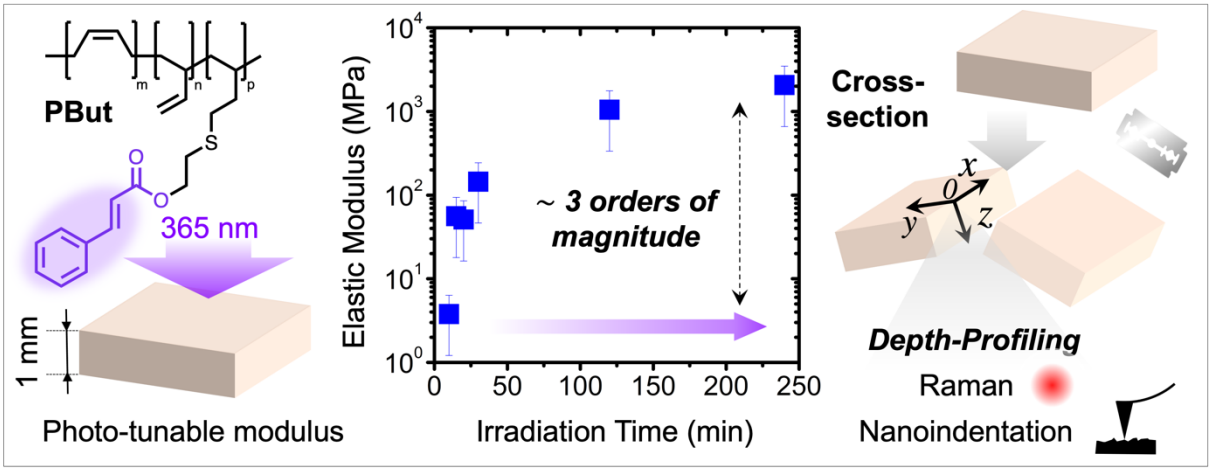

I. Introduction

Soft materials with an adjustable elastic modulus are crucial for various applications that demand precise control over viscoelastic properties, either over time or across different positions within an object.[1] Soft-robotics,[2] foldable electronics,[3] tissue engineering,[4] or metamaterials[5] are just a few examples of application fields where objects with evolutive mechanical response, in time and/or space, are needed. Cross-linked polymers, and in particular elastomers, offer a unique opportunity to achieve these objectives *via* the control of their cross-link density, or in other words the molecular weight, M_X, of the polymeric chains in-between the cross-linking point of their 3D network structure.[6] Strategies based on stimuli-responsive molecular systems to control M_X have been widely employed.[7-17] They include the use of polymers functionalized with light-responsive moieties.[10-18] In particular, photo-dimerizable molecules have been extensively used for the design of photo-crosslinkable polymers.[19-23] The most common systems are conjugated alkenes that can undergo a $[2\pi + 2\pi]$-cycloaddition reaction to form a cyclobutane ring under a given wavelength, usually UV-light (Figure 1A).[19, 20] Interestingly, most of these dimerization reactions are reversible upon application of an appropriate, shorter wavelength of light. Polymers bearing these conjugated alkenes can be cross-linked (*resp.* decrosslinked) under light irradiation, *via* the formation (*resp.* cleavage) of the dimers. The latter serve as the actual cross-linking points in the resulting elastomer (Figure 1B). Conveniently, the yield of the photo-dimerization reaction can be controlled *via* the light intensity and the irradiation time, in addition to all the conventional parameters that can affect their thermodynamic equilibrium and their kinetics (*e.g.* temperature, concentration, etc.).[11, 15,

[16] Playing with these two parameters is a simple strategy to control the cross-link density, and in return the mechanical response of the elastomers. An increase of the light intensity, or the irradiation time, results in a larger photo-dimerization yield. This comes with a decrease of M_X, *i.e.* an increase of the cross-link density and, consequently, of the Young modulus, E. Using directional beam of light, this strategy represents a simple, yet efficient, approach to control the mechanical performances of a soft material, both in time and space.

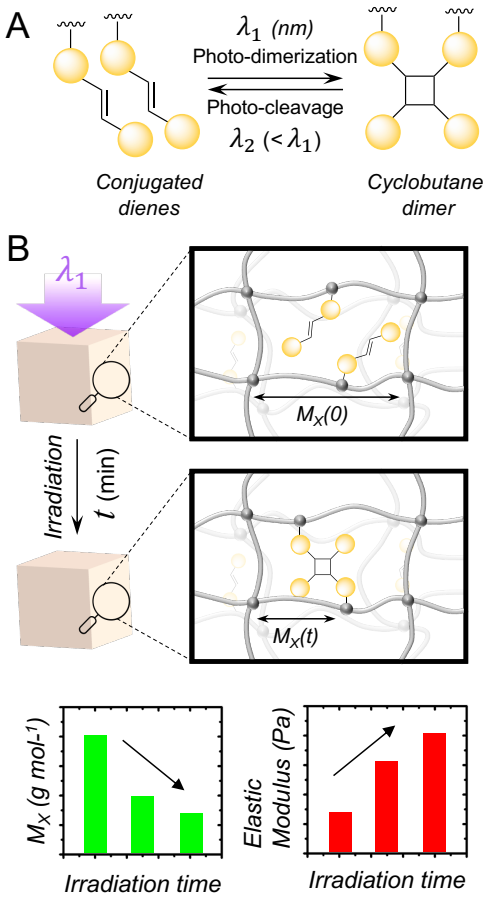

Figure 1: (A) Schematical representation of the photo-dimerization reaction of two conjugated alkenes *via* [2π + 2π]-cycloaddition reaction. Yellow circles represent aromatic rings and/or carbonylated moieties. (B) Schematical representation of the photo-control of the molecular weight in between crosslinking point, M_X, in a polymer network bearing photo-dimerizable moieties.

Classical photo-dimerizable moieties include cinnamoyl,[24, 25] coumarin[26, 27] or thymin[28] derivatives. Among them, cinnamoyl (Figure 2A) have been extensively used to fabricate photo-crosslinked polymer materials[11, 24, 25] and photo-crosslinked hydrogels.[29, 30] Advantageously, compounds containing cinnamoyl groups are often found in nature, especially in plants, and it has been proven that they are lowly toxic.[31] They undergo dimerization for wavelengths close to 360 nm, and the reversed reaction is observed around 265 nm. In a recent

example of the literature, Ito *et al.* conceived a polyester bearing cinnamoyl moieties, and used UV exposure for the easy tuning of the modulus, E, of the materials.[11] By controlling the exposure time in-between 0 and 30 min, they were able to tune the crosslink density of the material, and thus E over two orders of magnitude, $0.6 \leq E \leq 66$ MPa. Moreover, using photomasks, they were able to induce modulus patterning in a single monolithic sample, and to study the mechanical response of the sample in different directions relatively to the orientation of the pattern. This example illustrates well the potential of polymers functionalized with photo-dimerizable functions for the design of so-called smart materials. However, the use of light comes with some limitations related to the depth penetration of the radiation inside the materials. Indeed, the intensity of UV radiation, and thus the efficiency of the photo-dimerization reaction, decrease sharply as a function of depth.[14, 32-34] As a consequence, it is well accepted that it is difficult to achieve crosslinking in the bulk. For instance, in the above-mentioned example of Ito *et al.*, the authors used very thin samples (thickness = 0.1 mm) to ensure the homogeneous photo-crosslinking of the samples in the direction of the UV beam.[11] In a recent study, Averous *et al.* tried to estimate the maximum thickness of the film to guarantee a homogeneous photo-crosslinking.[14] Using a polyurethane functionalized with photo-dimerizable caffeic units, they irradiated samples of different thickness (0.2 mm to 1 mm) on one side, and compared the yield of the photo-dimerization reaction on both sides using FTIR spectroscopy in attenuated total reflection (ATR-FTIR). Interestingly, they showed that crosslinking takes place on the non-irradiated side, but only upon long exposure time. For instance, for a 0.2 mm thick film, they observed that, on the irradiated side, the photo-dimerization yield is maximal after only 10 min of exposure, while 16 h are necessary to observe the same yield on the non-irradiated side. Despite these intriguing results of the literature, the depth gradient of the crosslink density in bulk polymers bearing photo-dimerizable units has been very poorly investigated in the literature so far.

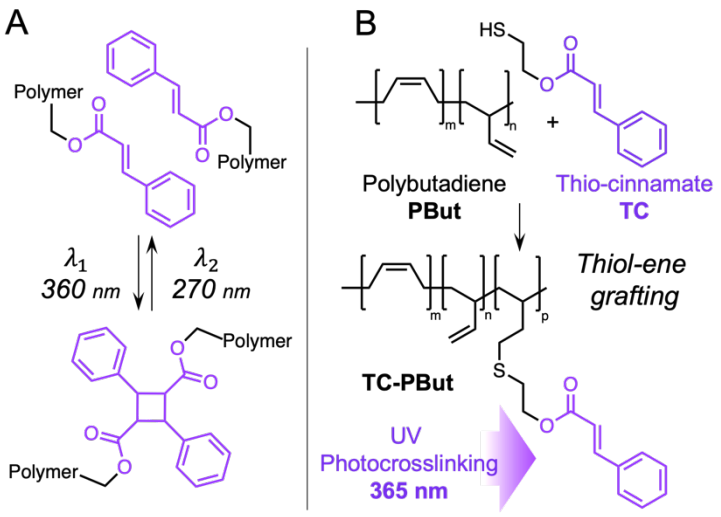

Figure 2: (A) Photo-dimerization reaction of two cinnamoyl groups at 365 nm and the reversed cleavage reaction at 270 nm, (B) Synthetic strategy used in this study: a thio-cinnamate ester (TC) is grafted onto a polybutadiene (PBut) *via* a thiol-ene reaction.

Herein, we functionalized a polybutadiene (PBut) backbone with pendent cinnamate ester groups, using thiol-ene click chemistry (Figure 2B). Other rubbers have been functionalized with cinnamate moieties in the past, essentially polyisoprene.[35-40] The grafting protocols developed so far were mostly based on the prior maleinisation of the rubber followed by ring-opening esterification of the maleic anhydride residue with oxyalkylcinnamate esters.[36-39] Other authors proposed to epoxidize the rubber, before ring opening the epoxy to provide hydroxyl groups that were further reacted with cinnamoyl chloride.[35] In all these works, the photo-polymerization was only investigated for the fabrication of thin films (< 0.2 mm), notably for biomedical applications.[35] In our study, the photo-crosslinking reaction of the functional PBut was investigated as a function of the exposure time, for millimeter thick samples (up to 2 mm). Remarkably, we demonstrated the possibility to vary the elastic modulus of the materials over almost three orders of magnitude (4 MPa $\leq E \leq$ 2 GPa), with relatively short exposure times (5 min $\leq t \leq$ 240 min). The photo-crosslinking kinetics were fully characterized, and more importantly, protocols were devised to probe the gradient of the yield of the photo-dimerization reaction, as well as the gradient of the elastic modulus, as a function of depth inside the millimeter-thick samples. After irradiation, the samples were sectioned and Raman spectroscopy was used to measure the photo-dimerization yield across the cross-section, for discrete points located at different distances of the irradiated surface. Similarly, Atomic Force Microscopy (AFM) nanoindentation was used to probe the local elastic modulus along the same

cross-sectional profile. The results indicate the existence of depth gradients, with moderated amplitudes. They suggest that the photo-dimerization reaction proceeds relatively well up to 1.5 mm beneath the irradiated surface, when the exposure times are comprised between 120 min and 240 min. In the end, they validate the possibility to use these photo-responsive rubbers as structural materials, with millimetric dimensions.

2. Experimental section

2.1. Materials and methods

Chemicals – Cinnamoyl chloride (98%, predominantly trans) was bought from Acros Organics. 2,2'-Azobis(4-methoxy-2,4-dimethylvaleronitrile) initiator (V70) was provided by Wako Chemicals. Polybutadiene (PB) (M_n = 3000 g/mol, 90% 1,2 vinyl) and 2-mercaptoethanol (98%) were provided by Sigma-Aldrich. Chloroform (HPLC grade), dichloromethane (0.2% of ethanol) and methanol technical were provided by VWR Chemicals and tetrahydrofurane (THF) was obtained from Scharlau. All chemicals were used as received.

FTIR – Fourier Transform InfraRed (FTIR) spectra were recorded on a Bruker-VERTEX 70 instrument (400 to 4000 cm^{-1}, 4 cm^{-1} resolution, 32 scans, DLaTGS MIR) equipped with a Pike GladiATR optical design diamond crystal) for attenuated total reflectance (ATR).

^{1}H NMR – NMR measurements (Bruker Advance) were carried out at 400 MHz, in $CDCl_3$ at room temperature from a 16 scans experiment, with a relaxation time of 1 sec.

Size exclusion Chromatography – Ultimate 3000 system (Thermoscientific) equipped with a diode array detector, a 3 multi-angles light scattering detector and differential refractive index detector (Wyatt Technology). Polymers were separated on three G2000, G3000 and G4000 TOSOH HXL gel columns (300 × 7.8 mm) (exclusion limits from 200 Da to 400,000 Da) with a flowrate of 1 mL/min at 40 °C and trichlorobenzene (TCB) used as a marker. The elution times were converted to molar mass using a conventional calibration curve based on PS standards (Agilent Kit - EasyVial PS-M 2mL).

Raman Spectroscopy – Raman measurements were performed with a XploRA spectrometer from Horiba using a laser source operating at 30 mW output power with a 785 nm excitation wavelength. The spectral resolution was about 3 cm^{-1} over a spectrum range from 900 to 1900 cm^{-1} using the grating 1200 lines/mm. In order to obtain a good signal to noise ratio, each spectrum results from the average of 3 accumulated scans with an integration time for each scan

of about 40 seconds. The laser beam was focused at the surface of the sample with the confocal microscope using a X10 objective.

Photo-Rheology – Photo-rheology was performed on a MCR rheometer from Anto Paar. The rheo-UV system consists of a temperature-controlled quartz plate and a UV light source with an attached light guide. UV-light is provided by a high-pressure 200 W mercury vapor short arc equipped with a filter for the emission of a discrete wavelength at 365 nm (7.28 W cm^{-2}). The temperature is controlled by a Peltier system.

Swelling test – Pieces of photo-crosslinked samples (thickness = 1 mm) were immersed for 48 h in THF at 50 °C. The variation of the sample mass was measured accurately by using a precision weighting scale. The gel content (GC) was measured as follow:

$$GC = \frac{m_1}{m_0} \times 100$$

where m_1 is the mass of the sample collected after 48 h of swelling in THF and dried for 48 h at 50 °C under vacuum.

The Swelling Ratio (SR) was obtained thanks to the following formula:

$$SR = \frac{m_s - m_1}{m_1} \times 100$$

in which m_s is the mass of the swollen sample after 48 h in THF.

Thermogravimetric Analysis – TGA analyses were performed on a Discovery TGA 550 from TA instrument. Samples (~ 10-15 mg) are placed in a platinum pan. Analyses are performed at a heating rate of 10 °C min^{-1} under a nitrogen (N_2) atmosphere from room temperature to 950 °C.

Differential Scanning Calorimetry – DSC analyses were performed on TA Instruments Q100 and Discovery 250. 5 to 15 mg of samples were sealed in an aluminum pan and analyzed under nitrogen flow. They were first cooled down to -80 °C then 3 cycles were performed between -80 °C and 150 °C at 10 °C min^{-1}. The glass transition temperatures reported in the study are extracted from the third cycle, *i.e.* the second heating cycle.

Dynamic mechanical analysis – The mechanical characterizations were conducted with a Discovery DMA850 apparatus from TA Instruments. The storage and loss moduli, *E'* and *E''* respectively, were measured at a frequency *f* = 1Hz and a strain ε = 0.1 % for T = 20 °C. Master

curves were constructed using the Time Temperature Super-position (TTS) principle, by measuring *E'* and *E''* for frequencies varying between 1 and 100 Hz (frequency sweeps), and with a strain ε = 0.005%. The shifting factors, a_T, were predetermined by shifting the different modulus-frequency curves as compared to a reference temperature, T_{ref}. Then the plot of the temperature dependance of the shifting factors, a_T, was fitted by using the WLF (Williams-Landel-Ferry) equation:

$$\ln(a_T) = \frac{-C_1(T - T_{ref})}{C_2 + (T - T_{ref})}$$

Where C_1 and C_2 are the shift factor parameters, T is the temperature and T_{ref} is the reference temperature as defined above. The shift factor parameters can then be used to calculate an adjusted value of the shifting factors, a_T, and the master curve is obtained by plotting *E'* against the reduced frequency as defined by $f_{ref} = f / a_T$. All data manipulations and calculations were performed with the software TRIOS from TA instrument. For all the samples the values of a_T (before and after adjustment), as well as the values of C_1 and C_2, are provided in the ESI.

Atomic Force Microscopy Nanoindentation – The samples are analyzed on a Bruker Dimension Icon device, operating in PeakForce Quantitative Nanomechanics (QNM) mode at room temperature. A calibration was performed using reference samples SAPPHIRE-12M (to calibrate the deflection sensitivity on a very hard surface) and PSFILM-12M (adjusting the tip radius to get a Young's modulus around 2.8 GPa at a given indentation depth) from Bruker. The force setpoint is then adjusted to obtain the modulus of the sample until the indentation depth is close to that obtained on PSFILM-12M (around 2 nm). The same indentation depth was used for all samples by adjusting the applied force based on the samples. PeakForce QNM produces force curves at 2 kHz from which mechanical data are extracted, *i.e.* the reduced Young's modulus by fitting the retract curve using the DMT model.[41] Each scanned image consists of 512 lines. Silicon tips (RTESPA-525-30) with a typical radius of 30 nm and a stiffness of 200 N m^{-1} are used. Images (*i.e.* Reduced Young's modulus maps) are obtained at a scan rate of 1 Hz.

2.2. Synthesis and preparation of the UV-crosslinked samples

Synthesis of the thio-cinnamate ester, TC – TC was prepared according to a procedure reported in the literature (ESI, Scheme S1).[25] In a round-bottom flask equipped with magnetic stirrer, cinnamoyl chloride (20 g, 120 mmol) was dissolved in toluene (300 mL). 2-mercaptoethanol (9.3 g, 120 mmol, 1 equiv.) was added dropwise and the mixture was stirred

under reflux for 2 hours. The solvent was removed on rotary evaporator to yield **TC** as a viscous liquid without any further purification. Yield= 90%. The structure and the purity of **TC** was confirmed by ^{1}H NMR spectroscopy (Figure S1).

Synthesis of the PBut functionalized with TC moieties, TC-PBut – **TC** was grafted on **PBut** *via* thiol-ene click chemistry (Figure 2B), using a protocol adapted from the literature.[25, 42, 43] A typical synthesis proceeds as follow: in a round-bottom flask equipped with magnetic stirrer, **PBut** was dissolved in chloroform (100 g L^{-1}), and **TC** was added (*X* equivalent compared to the C=C unsaturations). Then V70 was added (1 mol% compared to **TC**) and the reaction was allowed to proceed at 40 °C for 1 h. The polymer was then purified by precipitation in room temperature methanol and dried under vacuum. It was characterized by SEC and ^{1}H NMR. The number-averaged molecular weight (M_n), the weight-averaged molecular weight (M_w), and the dispersity ($Đ = M_w/M_n$) were measured by SEC. The structure of the resulting polymer as well as the grafting density, were investigated by ^{1}H NMR and FTIR spectroscopies, as well as by SEC chromatography.

UV-crosslinking of TC-PBut – The photo-crosslinked samples were obtained by pouring **TC-PBut** ($X = 0.5$) in a circular Teflon mold (Ø =30 mm, thickness 1 mm). This mold was enclosed in between two plates of quartz before exposure to UV light in a chamber equipped with UV LED System (KX-314-01, Novachem®, λ = 365 nm, 1000 mW cm^{-2}). Each side of the sample were exposed for the same amount of time, *t*, at 14 cm from the LEDs. The resulting samples are noted **TC-PBut-*t***. *t* was varied in-between 10 and 240 min. The resulting samples were investigated in FTIR spectroscopy, swelling tests, DSC and DMA. Forn the cross-sectional investigations, samples were photo-crosslinked in square molds (1 cm x 1 cm, depth = 2 mm) and only one side of the sample was irradiated as previously described. The resulting samples were sectioned, and their cross-section was surfaced by ultramicrotomy for Raman and AFM nanoindentation measurements.

Cross-sectioned samples preparation – Photo-crosslinked samples are cut with a razor blade. Then, they are placed on an aluminum vise and the fresh cross-section is surfaced using a Leica UC7 ultramicrotome equipped with a DIATOME TRIM, at a speed of 100 mm s^{-1} and a cutting thickness of 500 nm until the desired thickness is reached. To achieve the cleanest possible surface, the final surfacing is done with a DIATOME diamond knife at a speed of 1 mm s^{-1} and a cutting thickness of 50 nm. For the softer samples (UV exposure time of 10 min and 20 min), they were surfaced in a Leica UC7 cryo-ultramicrotome with a DIATOME TRIM and a

DIATOME diamond cryo-knife at -150 °C, with a speed of 1 mm s^{-1} and a cutting thickness of 70 nm.

3. Results and Discussion

Synthesis and characterization of TC-PBut

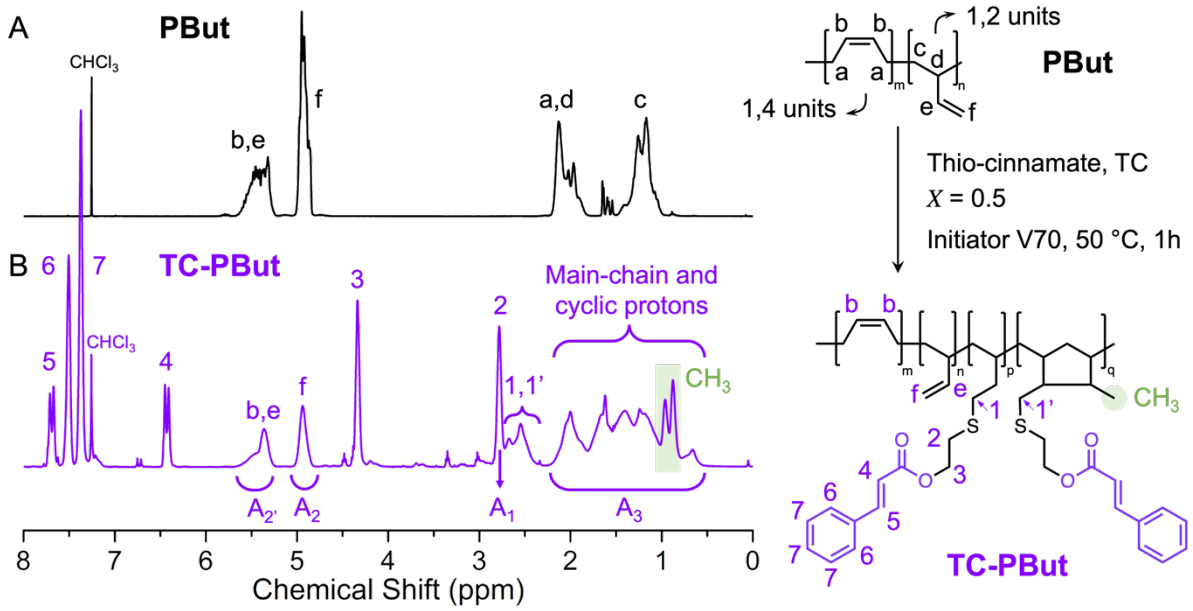

Figure 3: ^{1}H NMR spectra of (A) **PBut** and (B) **TC-PBut** for $X = 0.5$, showing the successful grafting of cinnamate functions and the concomitant cyclization reactions as attested by CH_3 signals in the downfield region (400 MHz, $CDCl_3$).

The **PBut** used in this study is a low molecular weight oligomer (M_n = 3600 g mol^{-1}) that is free of entanglement crosslinking (The critical entanglement spacing molecular weight of polybutadiene is closed to M_e ~ 6000 g mol^{-1}).[44] **TC-PBut** was synthesized according to a protocol adapted from the literature.[42, 43] In short, a thio-cinnamate ester, **TC**, was grafted on **PBut** *via* a thiol-ene click reaction, in the presence of a radical initiator (Figure 2B). Although this reaction was extensively used to functionalize **PBut** with a large variety of pendent groups, to our knowledge, it is the first time it is used to introduce cinnamate moieties. The grafting density can be controlled by varying X the number of equivalents of **TC** as compared to the number of C=C unsaturations, $X = [TC]_0/[C=C]_0$. In our experiments, we used X = 0.25 and 0.5. Figure 3B represents the ^{1}H NMR spectrum of **TC-PBut** for $X = 0.5$ (NMR spectrum of **TC-PBut** for $X = 0.25$ is reported in the ESI, Figure S2). It is compared to the NMR spectrum

of **PBut** prior grafting (Figure 3A). Clearly, the spectrum of **TC-PBut** is consistent with the efficient grafting of **TC** with the characteristic aromatic signals of the **TC** moieties. Moreover, in the low chemical shift region corresponding to the aliphatic protons, one can see signals below 1 ppm that can be attributed to methyl groups, CH_3. Their presence is well explained by the formation of ring structures *via* random cyclization of adjacent repeat units during the thiol-ene addition reaction as represented in Scheme 1. It is worth mentioning that two peaks can be distinguished. This multiplicity can be attributed to the coupling of the CH_3 protons with their CH neighbor. The unsymmetrical shape of the doublet might be attributed to the existence of different populations of CH_3 groups. Indeed, David *et al.* observed that the intramolecular cyclization reaction can propagate to form different polycyclic structures.[42] However, they demonstrated that the predominant one is the structure III, as represented in Scheme 1.

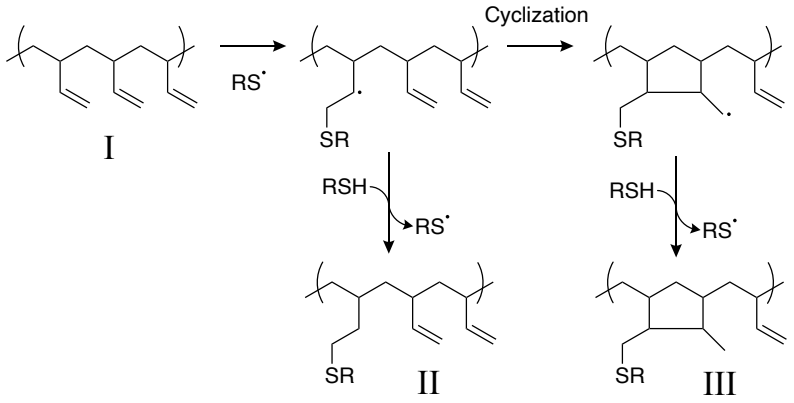

Scheme 1: Possible reaction pathways for radical thiol addition to 1,2-polybutadiene and competing cyclization reactions (RSH = **TC**)

The 1,4-C=C units being much less reactive than the 1,2 units, it can be approximated that they are not involved in the reaction. Let x_{funct} be the fraction of reacted **PBut** repeat units functionalized with a **TC** group (*i.e.* the grafting density), $x_{unreact}$ the fraction of unreacted repeat units, and x_{cycle} the fraction of reacted repeat units that are involved in a cyclization reaction. Then, by adapting a formalism that was first introduced by David *et al.*,[42] it is possible to calculate x_{funct}, $x_{unreact}$, and x_{cycle} from the integrals, A_1, A_2, $A_{2'}$, and A_3 from the RC**H₂**S- methylene protons (2), the **H₂**C=CH- alkenic protons (f), the -**H**C=C**H**- and H_2C=C**H**- alkenic protons (b, e), and the aliphatic protons (< 2.2 ppm), respectively (detailed calculation in the ESI, Figure S3). The calculated values are reported in Table 1. As expected, x_{funct} is an increasing function of *X*. Moreover, the results suggest that the number of 1,2-unsaturations functionalized with a **TC** moiety *vs* the number 1,2-unsaturations consumed by intramolecular

cyclization – without functionalization – are approximately the same. This is consistent with previous reports of the literature, where the cyclization to functionalization ratios x_{cycle}/x_{funct} are generally comprised between 1 and 1.5.[42]

Table 1: Molecular and thermal characteristics of **PBut** and **TC-PBut**'s

Entry	X [a]	x_{funct} [b] (mol%)	x_{cycle} [b] (mol%)	$x_{unreacted}$ [b] (mol%)	M_n [c] (g mol^{-1})	$Đ$ [c]	T_g [d] (°C)
1	0	-	-	-	3600	1.3	-27
2	0.25	17.1	23.3	59.5	4840	1.4	-18
3	0.50	33.0	33.5	33.5	5480	1.4	-11

[a] X is the number of equivalents of **TC** as compared to the number of C=C unsaturations of **PBut**, $X = [TC]_0/[C=C]_0$ used during the synthesis of **TC-PBut**. [b] x_{funct} is the fraction of reacted **PBut** repeat units functionalized with a **TC** group, $x_{unreact}$ the fraction of unreacted repeat units, and x_{cycle} the fraction of reacted repeat units that are involved in a cyclization reaction. They are calculated from the ^{1}H NMR spectrum of **TC-PBut** according to the methodology reported in the ESI. [c] The number average molar mass and dispersity as measured in SEC in THF. [d] Glass transition temperature as measured in DSC, 10 °C min^{-1}.

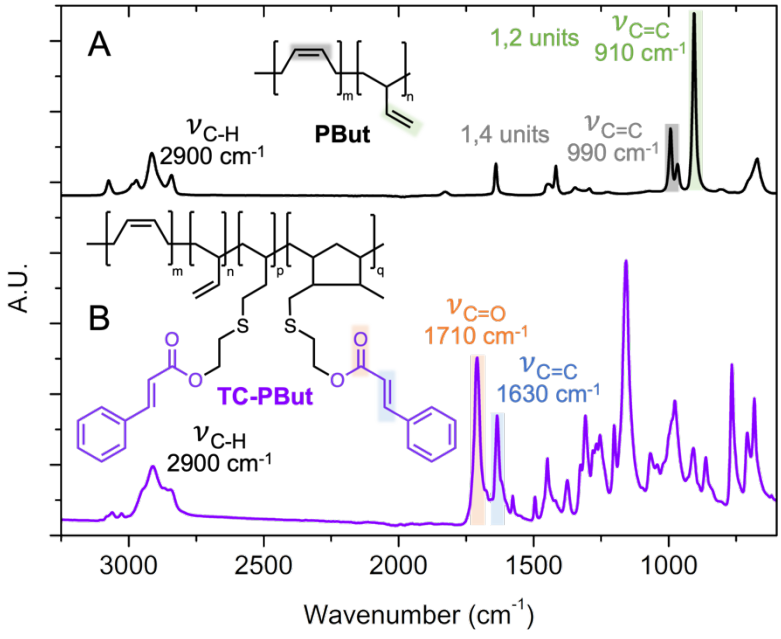

Figure 4: Infrared spectra of (A) **PBut** and (B) **TC-PBut** for $X = 0.5$, showing the successful grafting of cinnamate functions.

The good insertion of the cinnamic moieties onto the polymer backbone is also well confirmed by FTIR analysis. Figure 4 represents the FTIR spectrum of **TC-PBut** for X = 0.5, and it is compared to the FTIR spectrum of **PBut** prior grafting (FTIR spectrum of **TC-PBut** for X = 0.25 is reported in the ESI, Figure S4). Clearly, the presence of the cinnamate moieties in **TC-PBut** is attested by the distinctive stretching vibrations of the conjugated -C=O and -C=C- double bonds at $\nu_{C=O}$ = 1710 cm^{-1} and $\nu_{C=C}$ = 1630 cm^{-1}, respectively. The polymers were also characterized by size exclusion chromatography (SEC). The elugrams are presented in the ESI (Figures S5 to S7) and the corresponding values of the molar mass, M_n, and the dispersity, $Đ$, are reported in Table 1. This analysis further confirms the efficiency of the thiol-ene grafting reaction. Indeed, while **PBut** is not detected by the UV detector of the apparatus (Figure S5), **PBut-TC**'s display a saturated UV signal, consistent with their functionalization with the highly UV-responsive cinnamate moieties (Figures S6 and S7). As expected, M_n is an increasing function of X, which is consistent with the introduction of the cinnamate functions on the polymer backbone. It must be stressed out that M_n is calculated with respect to a polystyrene calibration and the values reported here are not absolute molar masses. Thus, cyclization also induces a modification of the hydrodynamic radius which may contribute, to some extent, to the apparent variations of M_n. Finally, the polymers were characterized by thermogravimetric analysis (TGA) and differential scanning calorimetry (DSC). TGA analysis indicates that the functionalization of **PBut** results in a reduction of the thermal stability of the polymer (Figure S8). Indeed, the temperature resulting in 5% of weight loss decreases from 392 °C for the pristine **PBut** to 299 °C for **TC-PBut**. This was expected because the thioether bonds introduced by thiol-ene chemistry are less stable than the hydrocarbon skeleton of the native polymer. The DSC thermograms are available in the ESI (Figure S9) and the corresponding values of the glass transition temperatures (T_g) are reported in Table 1. Again, T_g increases with X due to an increase of inter-chain interactions brought by the pendent cinnamic moieties, in particular through π-π interactions. Moreover, the intra-chain cyclizations are expected to increase the stiffness of the polymer chains by hampering the segmental motions and the molecular rotations.

In the end, despite the well-known drawbacks of the thiol-ene chemistry for the post-functionalization of polymers,[45] such as unintended non-specific radical reactions (as illustrated in this work) or the limitation of the long-term durability of the functionalized polymers (due to the limited stability of the thioether bonds), this methodology is an efficient approach to synthesize PBut functionalized with high grafting densities of photo-dimerizable moieties. For

comparison, in the literature, rubbers functionalized with cinnamic moieties, either through maleinisation[39] or epoxidation,[35] were usually reported with grafting densities varying from 2% to 15%. In the next parts of this study, the photo-crosslinking reactions were performed with the **TC-PBut** exhibiting the highest grafting density, *i.e.* x_{funct} = 33% (X = 0.5).

Rheometric monitoring of the photo-crosslinking reaction of TC-PBut

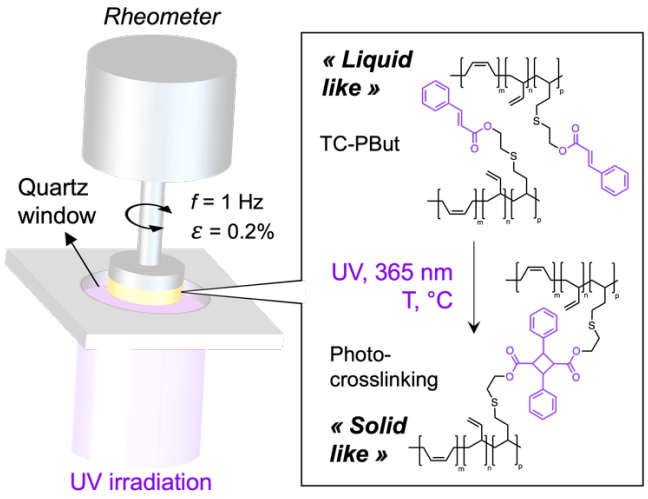

Figure 5: Schematical representation of the set-up used for the photo-rheological investigation of the UV-induced crosslinking reaction of **TC-PBut** and scheme of the photo-crosslinking reaction *via* the [2π + 2π] photo-cycloaddition of the cinnamic moieties, resulting in the transition from a "liquid like" polymer to a crosslinked gel (the *sol-gel* transition).

The photo-crosslinking reaction of **TC-PBut** was first investigated by photo-rheology to determine the best reaction conditions (Figure 5).[46] In this set-up, **TC-PBut** was charged in a rheometer equipped with a parallel plate geometry (diamater, Ø = 8 mm). The bottom part of the geometry is a quartz window allowing the exposition of the samples to UV light in the course of the measurements. Thus, the photo-crosslinking reaction can proceed while the samples is subjected to dynamic mechanical solicitations (oscillatory strain of amplitude ε = 0.2 % and frequency f = 1 Hz). Moreover, the temperature T of the system is regulated with a Peltier controller. In our experiment, the gap of the geometry is set to 0.5 mm to simulate the photo-crosslinking reaction of a millimeter-thick sample. UV light is delivered by a mercury vapor lamp equipped with a filter at λ = 365 nm. This experiment allows to measure the storage and the loss moduli, G' and G'' respectively, in the course of the photo-crosslinking reaction.

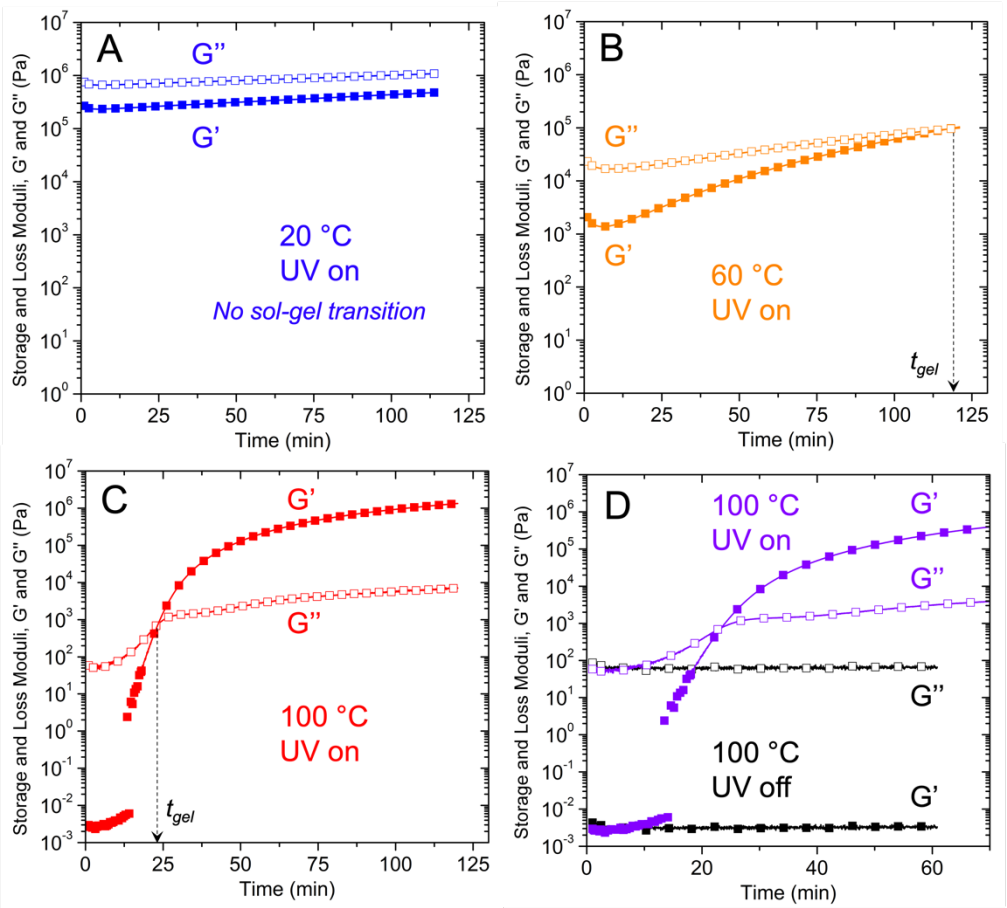

Figure 6: Evolution of the storage modulus (G', plain square) and the loss modulus (G'', open square) during the photo-crosslinking reaction of **TC-PBut** ($X = 0.5$) as investigated by photo-rheology ($f = 1$ Hz, $\varepsilon = 0.2\%$) under UV irradiation at 365 nm and for different temperatures: (A) T = 20 °C, (B) T = 60 °C, (C) T = 100 °C, (D) T = 100 °C, comparison of conditions with and without UV irradiation.

Figure 6A represents the monitoring of the photo-crosslinking reaction at T = 20 °C. Clearly, G' < G'' during the whole duration of the experiment (120 min), meaning that the exposure to UV light is not sufficient to observe the formation of a well crosslinked polymer network. The temperature was then increased to T = 60 °C (Figure 6B). In this case, the onset of a *sol-gel* transition (G' = G'') is observed for $t_{gel} \sim 120$ min, where t_{gel} is the gel time. Further increase of the temperature to T = 100 °C results in a substantial decrease of t_{gel} to 23 min (Figure 6C). These first experiments demonstrate that it is possible to photo-crosslink a 0.5 mm-thick sample and that temperature is fostering the process. It is worth mentioning that the reference experiment performed at 100 °C without UV exposure (Figure 6D), indicates that **TC-PBut** is not crosslinked in these conditions, thus confirming that the *sol-gel* transition requires the simultaneous action of temperature and UV illumination. Temperature is expected to help in increasing molecular motion and thus, in enhancing the encountering and the alignment of two

neighboring cinnamate functions, that is required to observe the cycloaddition reaction.[47] In the end, this initial series of experiments successfully demonstrates the potential to crosslink millimeters-thick samples. However, they do not provide any insight into the depth gradient of crosslink density within the samples. A comprehensive spectroscopic analysis was conducted to investigate this aspect.

Spectroscopic monitoring of the photo-crosslinking reaction of TC-PBut

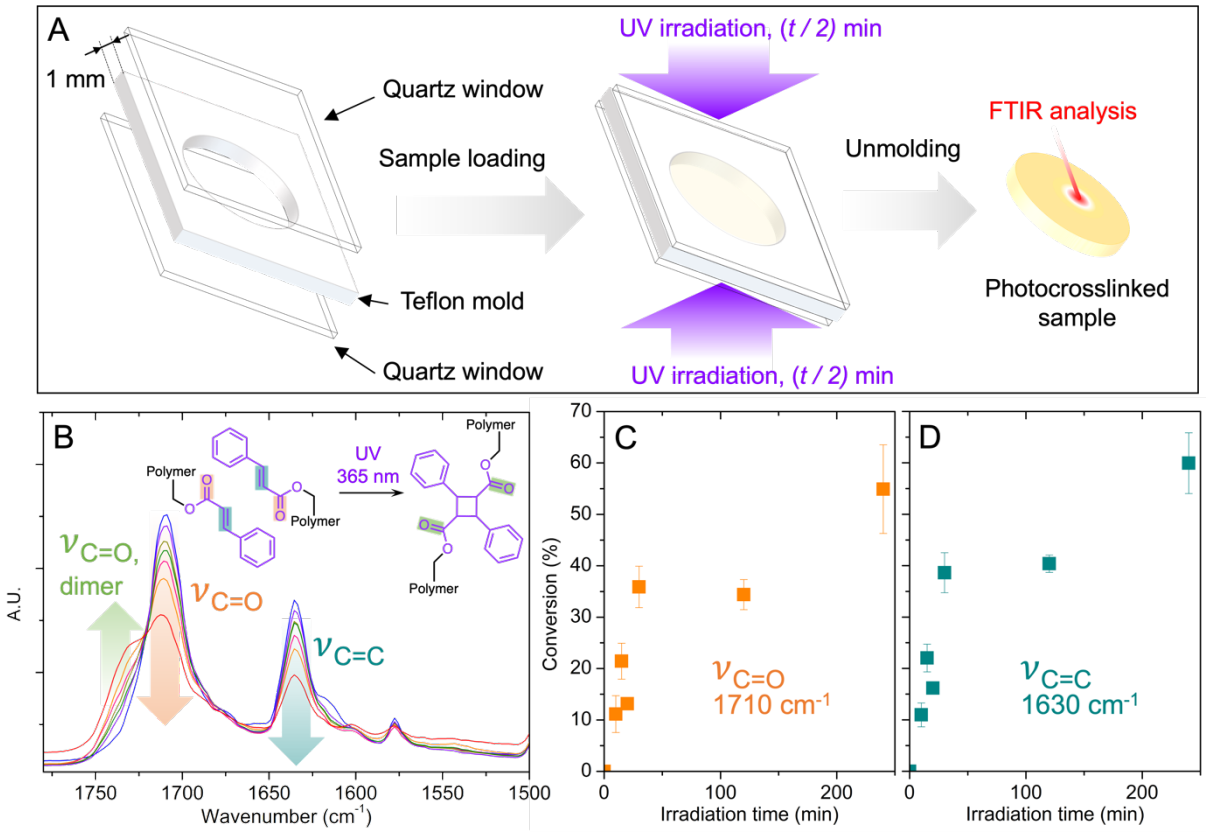

Figure 7: (A) Schematical representation of the design of the sandwiched mold used for the fabrication of the photo-crosslinked samples investigated in ATR-FTIR analysis, in swelling tests and in dynamic mechanical analysis. (B) Evolution of the FTIR spectra as a function of UV irradiation time (365 nm), for the photo-crosslinking reaction of TC-PBut (X = 0.5). Spectra were magnified in the region corresponding to the bands of the C=O elongation, $\nu_{C=O}$, at 1710 cm^{-1} and the C=C elongation, $\nu_{C=C}$, at 1635 cm^{-1}. (C) and (D) Evolution of the conversion of cinnamic moieties into dimers as a function of the UV irradiation time, as calculated from the intensity of the C=O elongation band and the C=C elongation band, respectively.

We first investigated the kinetics of the photo-crosslinking reaction using FTIR in Attenuated Total Reflectance mode (ATR), meaning that only the surface of the sample was probed. The samples prepared for analysis were obtained by pouring the polymer in a circular cell made of a Teflon mould (1 mm thick) maintained in-between two quartz windows (Figure

7A). They were exposed to UV for a total duration of *t* min, both side of the cell being irradiated for the same amount of time, *i.e.* *t*/2 min. *t* was varied in between 5 and 240 min, and the resulting samples are noted **TC-PBut-*t***. The UV system is a chamber in which only the power of the LED array can be controlled. The temperature is not regulated. However, due to the strong power of the LED (1000 mW cm^{-2}), it is observed that the samples are heated up by UV radiation. In the present study, a thermocouple was used to measure the temperature of the sample during exposure. A plateau is quickly reached around 120 °C in ~ 5 min (Figure S10). Conveniently, based on the results obtained in photo-rheology, this temperature increase is sufficient to observe an efficient photo-crosslinking reaction. It is worth noting that, the impact of temperature on the photo-crosslinking rate of polymers bearing photo-dimerizable moieties is poorly addressed in the literature and the temperature increase induced by the irradiation is usually not reported.

Figure 7B represents the evolution of the FTIR spectra of the samples as a function of *t*. In accordance with previous reports of the literature,[35, 48] the bands corresponding to the C=O elongation, $\nu_{C=O}$, at 1710 cm^{-1} and the C=C elongation, $\nu_{C=C}$, at 1635 cm^{-1} are clearly impacted by UV irradiation. $\nu_{C=C}$ progressively decreases while $\nu_{C=O}$ is shifted to longer wavelength, which is consistent with the photo-induced dimerization of the C=C double bonds, and the resulting new chemical environment for the C=O carbonyl bonds. $(I_\nu)_0$, the initial intensity of the ν band and $(I_\nu)_t$, the intensity after UV exposure during *t* min, can be used to measure the conversion of cinnamate moieties into the corresponding dimer. Both values were normalized by the intensity of the band attributed to the vibration of the C-H bonds of the carbon of the main chain, at 2915 cm^{-1} (*cf.* the full-scale spectrum, Figure 4). Then, the conversion can be calculated *via* the following equation: $[((I_\nu)_0 - (I_\nu)_t)/ (I_\nu)_0] \times 100$.

Figures 7C and 7D represent the evolution of the conversion using the $\nu_{C=O}$ and the $\nu_{C=C}$ vibrations, respectively. Both graphs exhibit the same trend with first a steep increase between 0 and 30 minutes, followed by a relatively slower evolution of the conversion at larger time. The conversion rate seems to reach a plateau around 60% in both cases. Interestingly, in their study of photo-crosslinkable polyisoprene functionalized with cinnamate moieties, Derouet *et al.* observed a very similar behavior, with a conversion plateau around 60 %. This was explained by the decrease of chains mobility, due to the three-dimensional network formation which reduces the probability of cinnamate groups encountering. As expected, varying the irradiation time in-between 10 and 240 min is a simple approach to control the conversion of the dimerization reaction and thus, the crosslinking degree of the material.

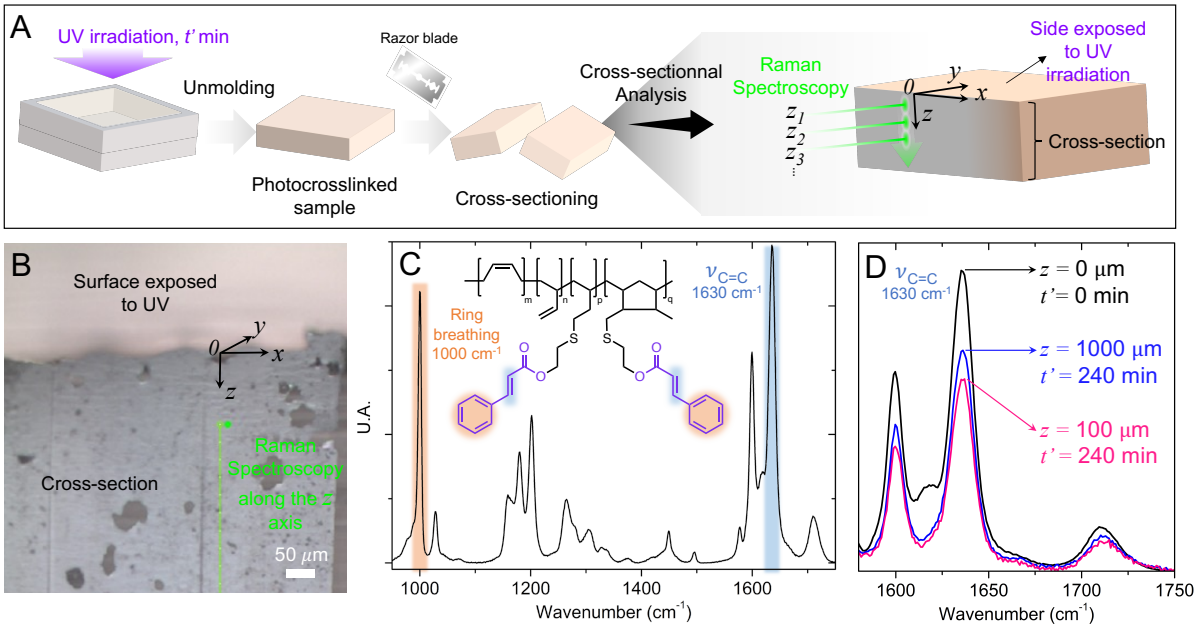

Figure 8: (A) Schematical representation of the preparation of the photo-crosslinked samples for their cross-sectional investigation by Raman spectroscopy and AFM measurements. (B) Picture of a typical cross-section investigated by Raman spectroscopy in different points located along the *z*-axis (**TC-PBut**, $X = 0.5$). (C) Full Raman spectrum of **TC-PBut** ($X = 0.5$) with band attribution. (D) Raman spectra collected at various depth, on sample exposed for different duration, *t'*. Black spectrum: (z, *t'*) = (0 μm, 0 min), blue spectrum: (z, *t'*) = (1000 μm, 240 min), pink spectrum (z, *t'*) = (100 μm, 240 min). Spectra are magnified in the region corresponding to the bands of the C=C elongation, $\nu_{C=C}$, at 1630 cm^{-1}. They are all normalized by the intensity of the band corresponding to the "ring breathing" of the phenyl groups at 1000 cm^{-1}.

In order to go deeper in the understanding of the system, the evolution of the gradient of the conversion as a function of depth, inside the bulk of the sample, was investigated through Raman spectroscopy. To our knowledge, this was never considered for the photo-crosslinking reaction of polymers bearing photo-dimerizable moieties. The objective is two-fold: (i) quantify the efficiency of the photo-crosslinking reaction inside the material, and (ii) evaluate its impact on the thermo-mechanical properties. To do so, samples were crosslinked using the methodology reported earlier (1000 mW cm^{-2}, 14 cm from the LED source). Only one face of the sample was exposed to simplify the interpretations of the results. The photo-crosslinked polymers were then sectioned, and the conversion was investigated locally, along the cross-section, using Raman microscopy (Figure 8A). Spectra were collected along the z axis, at various depth, on sample exposed for different durations, *t'*, with *t'* = 10, 20, 120 and 240 min. The picture of a typical cross-section, acquired by optical microscopy, is displayed in Figure

8B. The very smooth surface was guaranteed by surfacing the cross-section *via* ultramicrotomy (cf. *Materials and Methods* section). Figure 8C represents the Raman spectrum of **TC-PBut** (X = 0.5), prior UV irradiation (t' = 0). From the literature, it is known that the strong band at 1630 cm^{-1} is associated to the stretching mode of the C=C double bond of the cinnamate group, while the strong band at 1000 cm^{-1} is associated to a vibration mode of the phenyl rings ("ring breathing").[49] The latter was used for the normalization of the spectra collected at various depth, z, and time, t'. Figure 8D displays the spectra for (z, t') = (0 μm, 0 min), (z, t') = (100 μm, 240 min), and (z, t') = (1000 μm, 240 min), with a magnification in the region corresponding to the bands of the C=C elongation, $\nu_{C=C}$, at 1630 cm^{-1}. Clearly, for t' = 240 min, the intensity of the $\nu_{C=C}$ band decreases for both depth, z = 100 μm and 1000 μm, which is consistent with the progress of the photo-crosslinking reaction. Moreover, the intensity of the same band increases from z = 100 μm to z = 1000 μm, thus suggesting a decreasing extent of the reaction as the distance from the surface increases. This is in accordance with a reduction of the UV penetration as a function of z. The conversion of the cinnamate groups into dimers was calculated using the equation: $[((I_{C=C})_0 - (I_{C=C})_{t'})/ (I_{C=C})_0] \times 100\%$, where $(I_{C=C})_0$ is the initial intensity of the band at 1630 cm^{-1}, and $(I_{C=C})_{t'}$, the intensity after UV irradiation during t min, both being normalized by the intensity of the band at 1000 cm^{-1}.

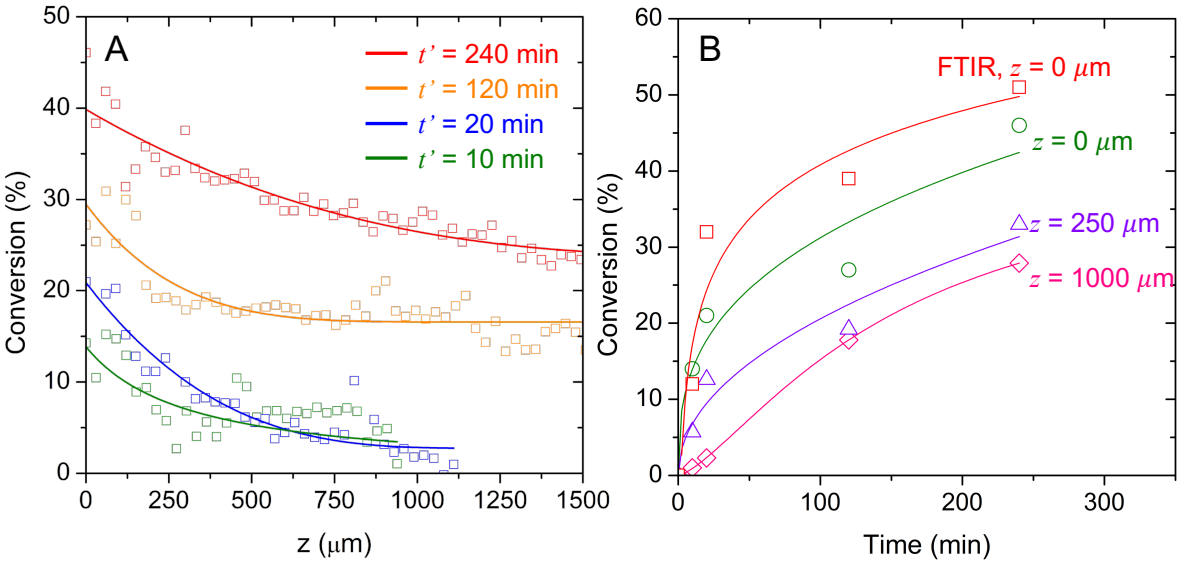

Figure 9: (A) Evolution of the conversion of cinnamate moieties into dimers as a function of the distance z (depth) beneath the surface of the sample exposed to UV for different irradiation time, t'. (B) Evolution of the conversion of cinnamate moieties into dimers as a function of the UV irradiation time for different distances z (depth) beneath the surface of the sample exposed to UV. In both cases, the data are extracted from the Raman measurements using the intensity of the C=C elongation band for **TC-PBut**, X = 0.5. In panel (B) the red curve (squares) represents the conversion as measured in FTIR, for comparison with the results of Raman spectroscopy. The lines are guides for the eye.

Figure 9A represents the evolution of the conversion as a function of z for the different exposure times. As expected, the conversion is a decreasing function of z and an increasing function of t'. For all the irradiation times, one can note that the conversion decreases significantly in the first 0.25 mm, before a regime with a much slower decline. For t' = 10 min and 20 min, the conversion decreases down to ~ 0% for z ~ 1 mm. This is in accordance with the experimental observations. Indeed, in both cases, a significant amount of the sample remained in the 2 mm-thick mold after unmolding. The actual thickness of the photo-crosslinked samples was ~ 1 mm, and the non-irradiated side was very sticky, thus confirming that the sample was not photo-crosslinked for z larger than 1 mm. For longer irradiation times of 120 and 240 min, samples with a thickness of approximately 1.5 mm were successfully unmolded. Some of the polymer remained adhered to the mold, although it appeared crosslinked (non-tacky). This suggests that the loss of material was likely due to difficulties in removing the polymer from the mold rather than an incomplete photo-crosslinking reaction at these depths. Accordingly, it was possible to measure the conversion down to z ~ 1.5 mm, with substantial values of ~16% and ~24%, for t' = 120 min and 240 min, respectively. These results indicate that the photo-crosslinking reaction still proceeds relatively well 1 mm beneath the surface for exposure times > 2h. Moreover, although these profiles confirm a heterogeneously crosslinked material in thickness, the depth gradients are of moderated amplitudes. Indeed, the difference between the conversion at z = 0 and z = 1 mm is of ~ 14 % for t' = 120 min, and ~ 9 % for t' = 240 min. Similarly, Figure 9B represents the time dependence of the conversion for discrete values of z, z = 0, 0.25 and 1 mm. It confirms that the larger differences of conversion are observed within a 0.25 mm deep region from the irradiated surface. For comparison purposes, the surfaces of these samples were also analyzed by ATR FTIR. The evolution of the conversion as a function of time is reported in Figure 9B, along the results obtained by Raman spectroscopy. It looks like the values obtained by FTIR analysis are slightly higher than those measured by Raman spectroscopy for z = 0. However, given that the two methodologies are probing the surface of the sample in very different manners (scattering for Raman *vs* evanescent wave for FTIR), this difference is not surprising. Overall, the results suggest a good consistency between the two experimental approaches. Before going any further in the comparison of the thermomechanical properties of the samples, they were first engaged in swelling tests to evaluate the efficiency of the photo-crosslinking reaction in terms of gel fraction.

Swelling tests

With the appreciation of the existing heterogeneities inside the photo-crosslinked polymers, it was of interest to investigate their swelling behavior in a good solvent. Indeed, swelling tests are commonly performed to assess the efficiency of crosslinking reactions (both thermo- and photo-induced). In particular, the measurement of the gel content (GC) was used by several authors to evaluate whether 0.1 to 0.5 mm thick samples were photo-crosslinked across the entire thickness.[15, 35] Here, we used the 1 mm thick samples obtained by exposing the two sides of the samples to UV irradiations (Figure 7A), a portion of which was extracted by THF for 2 days at 50 °C. The weight of material was measured before extraction and after extraction both in the wet and dry state. The gel content was calculated as the weight percentage of insoluble polymer relative to the initial mass of polymer.

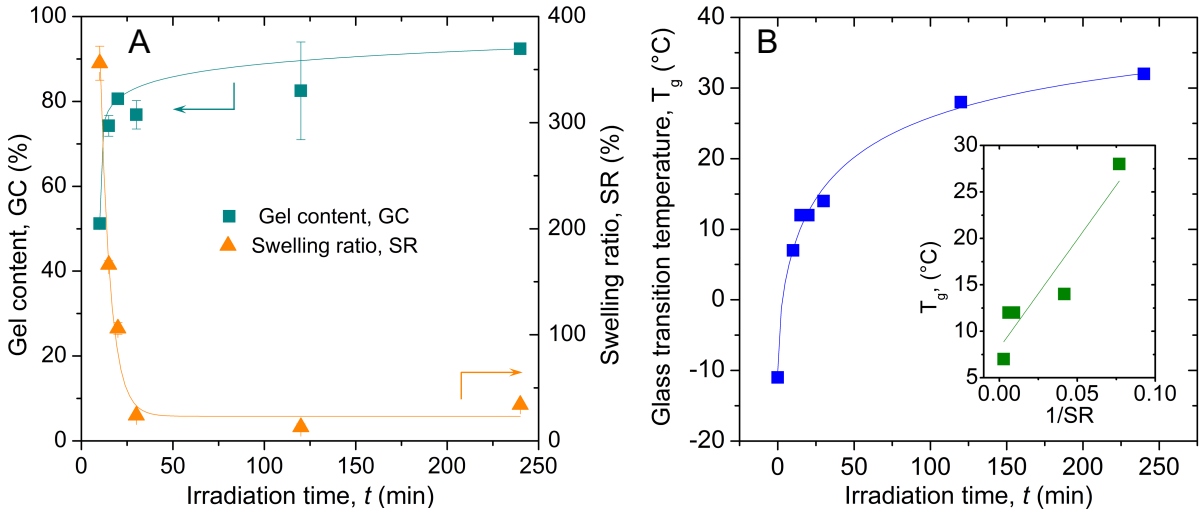

Figure 10: (A) Evolution of the Gel Content (GC) and the Swelling Ratio (SR), and (B) evolution of the glass transition temperature (T_g), as a function of the UV irradiation time, *t*, for **TC-PBut-*t*** samples (X = 0.5, thickness = 1 mm). The lines are guides for the eye. The insert of panel (B) represents the evolution of T_g versus the inverse of SR, 1/SR.

GC values are reported in Table 2 and Figure 10A represents the evolution of GC versus the irradiation time *t*. The gel content rapidly increases with *t* and plateaus around 80-90%. Similar values were reported for 0.5 mm samples of polyisoprene bearing cinnamate moieties.[35] They indicate that the networks are very well crosslinked. It is only for the shortest exposure time, t = 10 min, that the value of GC is relatively small, ~ 50%. By comparing this result with the conversion degree measured in Raman spectroscopy, it can be approximated that a threshold value of ~10% conversion, across the whole sample, is a good guarantee for an efficient photo-

crosslinking reaction. Indeed, based on the depth profiles of the conversion (Figure 9A), for a 1 mm thick sample exposed on both sides for 10 min, the conversion at the core of the material, *i.e.* for z = 0.5 mm, should be ≳ 10%. In the end, the gradient of conversion observed in Raman spectroscopy are not an obstacle to the efficient photo-curing of the 1 mm thick samples for exposure times ≥ 20 min. The evolution of the swelling ratio, SR, as a function of *t* is plotted in Figure 10B. SR is large (> 100%) for *t* comprised between 10 and 30 min, which is in accordance with the low crosslink density of these loose networks, and it reaches a plateau around 30% for longer irradiation time. Thus, the evolution of SR validates the possibility to change the crosslink density by varying *t*.

Table 2: Data related to the swelling investigations and the thermomechanical properties of the **TC-PBut-*t*** (*X* = 0.5, thickness = 1 mm) samples photo-crosslinked for *t* min under UV irradiation (365 nm).

Sample	*t*/2 [a] *(min)*	*GC* [b] (%)	*SR* [b] (%)	T_g [c] (°C)	*E'* [d] (MPa)
TC-PBut-0	0	-	-	-11	-
TC-PBut-10	5	51	356	7	3.8
TC-PBut-15	7.5	74	166	12	56
TC-PBut-20	10	81	106	12	51
TC-PBut-30	15	77	24	14	145
TC-PBut-120	60	82	13	28	1050
TC-PBut-240	120	92	34	32	2070

[a] Exposure time to UV irradiation (365 nm), each side of the sample are exposed to *t*/2 min. [b] Gel Content and Swelling Ratio as measured from swelling tests in THF (50 °C, 2 days). [c] Glass transition temperature as measured in DSC, 10 °C min^{-1}. [d] Dynamic storage modulus as measured in DMA (T = 20 °C, *f* = 1 Hz, ε = 0.005 %).

Glass transition temperatures

Having fully characterized the efficiency of the photo-crosslinking reaction, we then investigated the evolution of the physical properties of the elastomers depending on the irradiation time, *t*. First, we measured the glass transition temperature, T_g, by DSC. For all the exposure times, the DSC thermogram of the corresponding samples is represented in the ESI, Figures S15 to S16. It must be stressed out that, for this analysis, very small amounts of samples are analyzed (5 to 15 mg) and it is not possible to consider pieces of materials that are

representative of the whole thickness. However, different zones of the samples were analyzed, and we never observed any transition that would suggest a strongly inhomogeneous structure (no double-transition or such). Figure 10B represents the evolution of T_g with t. It increases moderately for t varying from 10 to 30 min, before surpassing room-temperature for t = 120, and 240 min. Overall, by increasing the photo-crosslinking time, it is possible to explore a T_g range, ΔT_g, of ~ 25 °C and to vary from a rubbery to a glassy behavior at room temperature. In the previous studies of the literature dedicated to rubbers bearing cinnamate functions, the T_g was not impacted by the photo-crosslinking reaction, most likely because the functionalization degree was much lower (5-10%).[35] For other polymer families, such as polyurethane, ΔT_g's of ~ 10 °C are classically reported.[11] It is interesting to note that the Fox-Loshaek equation[50] correlates the T_g values to the crosslink density *via* the formula: $T_{g(network)} = T_{g(linear)} + k \times \nu$, where $T_{g(network)}$ and $T_{g(linear)}$ are the glass transition temperatures of the crosslinked and uncrosslinked material, *i.e.* **TC-PBut-0** and **TC-PBut-*t***** respectively, k a factor depending on the network rigidity and ν the crosslink density. Although it is difficult to estimate the accurate crosslink density of these networks due to the missing information regarding the Flory-Huggins solvent-polymer interaction parameters,[51] it is well known that ν is inversely proportional to the swelling ratio SR. Thus, we tentatively plotted the evolution of ΔT_g *vs* the inverse of *SR*, where $\Delta T_g = T_g$ (**TC-PBut-*t***) - T_g (**TC-PBut-*0***). It is represented in the insert of Figure 10B. Despite the small number of data points, the tendency is compatible with a sharp linear increase of ΔT_g as a function of 1/SR, as suggested by the Fox-Loshaek equation. Thus, the control of the crosslink density *via* the irradiation time is well validated by the experimental measurements of SR and T_g.

Mechanical properties

Ultimately, we went on to investigate the mechanical properties of the **TC-PBut** samples as a function of the irradiation time, t. The tensile storage modulus, *E'*, was first measured by dynamic mechanical analysis at 1 Hz (ε = 0.005%) and 20 °C. For all **TC-PBut-*t*** samples, the values of *E'* are reported in Table 2, and the evolution of *E'* as a function of t is plotted in Figure 11A. *E'* increases upon t increase, in accordance with the expected evolution of the crosslink density. Remarkably, *E'* values vary from 3.8 MPa for t = 10 min to 2070 MPa for t = 240 min, meaning that it is possible to explore two orders of magnitude in terms of storage modulus, simply by varying the irradiation time. To our knowledge, in the literature dedicated to materials with tunable modulus, only one study reported such a wide amplitude at room temperature (~ 20 °C).[11] It must be stressed out that *E'* is directly related to the crosslink

density only in the rubbery domain, notably *via* simple models such as the rubber elasticity theory.[52] In the glassy domain, *E'* becomes dependent on segmental mobility and there is no trivial model to predict its evolution. With this consideration in mind, the very large amplitude of the storage modulus of our system observed upon irradiation, is due to a synergetic effect of the increase in both the cross-link density and the T_g, the latter becoming predominant for the long exposure times. Indeed, the very large increase of *E'* observed for **TC-PBut-120** and **TC-PBut-240** is essentially due to the increase of their T_g beyond 20 °C, the temperature of the measurements. Ito *et al.* made a similar observation during their study of a photo-crosslinkable polyester bearing cinnamate moieties.[11]

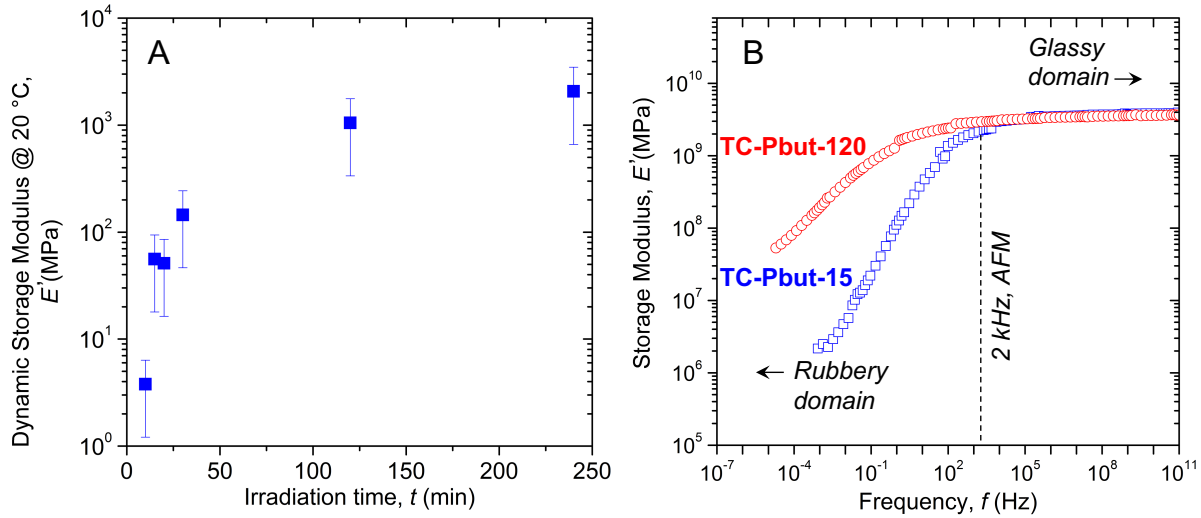

Figure 11: (A) Evolution of the tensile storage modulus, *E'*, as a function of the UV irradiation time, *t*, for **TC-PBut-*t*** samples (X = 0.5, thickness = 1 mm), as measured in DMA (f = 1 Hz, ε = 0.1 %, T = 20 °C). (B) Evolution of the tensile storage modulus of **TC-PBut-15** and **TC-PBut-120**, as a function of the frequency. These master curves were obtained using the Time Temperature Superposition Principle.

In order to test further the consistency of our results with the expected evolution of the crosslink density, the mechanical properties of **TC-PBut-15** and **TC-PBut-120** were investigated in DMA *via* frequency sweeps, from 1 Hz to 100 Hz, at various temperatures comprised between -50 °C and 50 °C. Using the Time Temperature Superposition Principle,[53] it is possible to construct a viscoelastic master curve to represent the evolution of *E'* as a function of frequency, *f*. Figure 11B represents *E'* plotted against the reduced frequency (f_{ref}) varying from 10^{-4} to 10^{10} Hz (Detailed procedure in the *Materials and Method* section, Figure S17 and S18, and Table S2 to S5). In this plot, decreasing frequency is equivalent to increasing temperature, and inversely. At high frequencies ($f > 10^3$ Hz), one can see the glassy plateau.

The corresponding glassy modulus is approximately the same for both samples, E_g ~ 3.5 GPa. This was expected given that, in this region, the molecular motions are blocked, and the crosslink density has a limited impact on the value of the modulus. At low frequencies, *i.e.* in the rubbery domain, the two master curves exhibit very different slopes, which reflects the difference in terms of crosslink density in-between the two polymers. As expected, E is much higher in the case of **TC-PBut-120**, the sample irradiated for the longer time. It is worth noting that, for both materials, we were not able to observe the rubbery plateau in the conditions of our experiments. However, the value of the storage rubbery modulus, E'_r, can be estimated by considering the frequency sweeps performed at temperatures well above the T_g of the materials, *i.e.* T = 40 °C for **TC-PBut-15** and T = 50 °C for **TC-PBut-120** (Figure S17 and S18). We found E'_r = 2.2 MPa and 53 MPa at 1 Hz for **TC-PBut-15** and **TC-PBut-120**, respectively. In the frame of the rubber elasticity theory,[52] E'_r is directly proportional to the molecular weight between crosslink, M_X:

$$E'_r = \frac{3\rho RT}{M_X}$$

Where ρ, R and T represent the polymer density, the gas constant, and the measurement temperature, respectively. ρ was measured with a pycnometer (*ca.* 1.1 g cm^{-3}). With these values in hand, one can calculate M_X = 3900 and 160 g mol^{-1}, for **TC-PBut-15** and **TC-PBut-120**, respectively. Considering the molecular weight of **TC-PBut** prior photo-crosslinking as measured in SEC, M_n = 5480 g mol^{-1}, we have: M_X(**TC-PBut-120**) < M_X(**TC-PBut-15**) < M_n(**TC-PBut-0**). This evolution is consistent and validates well the control of the crosslink density *via* UV-irradiation.

In line with the Raman investigation of the dimerization conversion as a function of depth, a gradient of elastic modulus was anticipated across the millimeters-thick samples. Thus, we decided to probe the in-depth evolution of E' along the cross-section of photo-crosslinked samples. To our knowledge, this was never done for UV-crosslinkable polymers bearing photo-dimerizable units. Previous works of the literature undertook the in-depth profiling of the mechanical properties in polymeric coatings,[54-56] notably to quantify the impact of UV-photodegradation.[56] In these studies, atomic force microscopy (AFM) nanoindentation[57-59] is the preferred method for the local measurement of the elastic modulus on micrometric areas.[60, 61] Herein, we tentatively implemented this methodology to measure E'_{AFM}, the storage modulus, beneath the surface exposed to UV during the photo-crosslinking reaction (detailed procedure in the *Materials and Method* section). Cross-sectioned specimens were prepared following the

procedure used for the Raman spectroscopy investigations (see Figure 8A). First, they were analyzed close to the irradiated surface (z = 100 μm). Figure 12A represents the evolution of E'_{AFM} as a function of the irradiation time, t. The corresponding Young's modulus mapping are reported in the ESI, Figures S19 to S22.

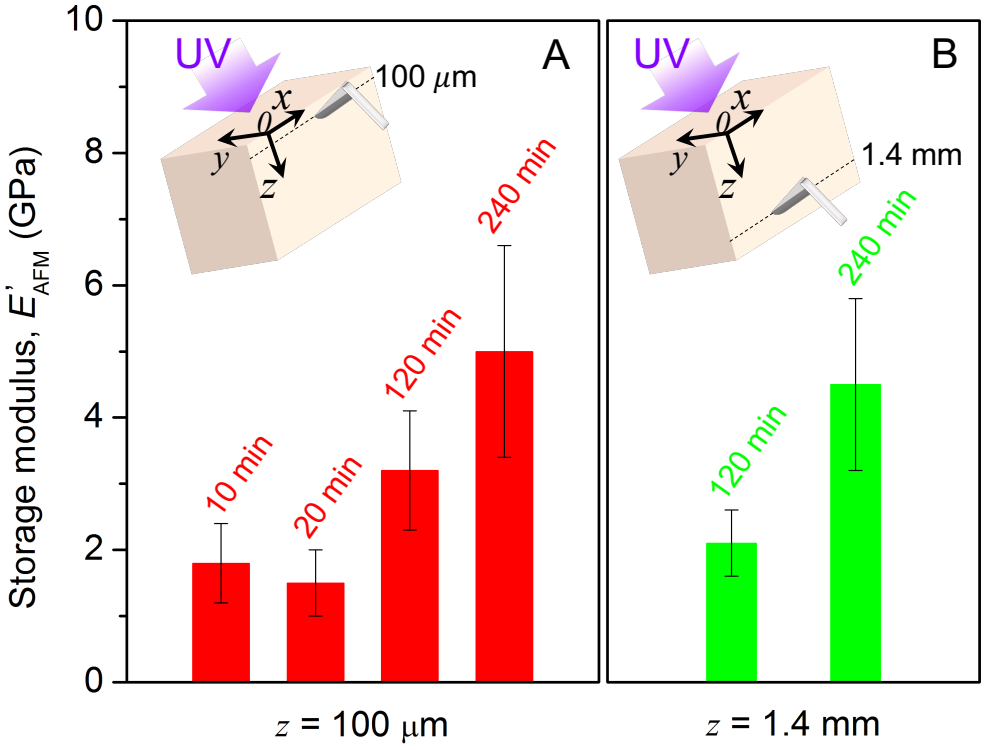

Figure 12: Evolution of the storage modulus, E'_{AFM}, measured by AFM nanoindentation (f = 2 kHz), as a function of the irradiation time, t, for two distances beneath the surface of the irradiated side: (A) z = 100 μm, and (B) z = 1400 μm.

E'_{AFM} is an increasing function of t, in accordance with the expected evolution of the crosslinking density. One can note that for t = 10 min and 20 min, E_{AFM} ~ 1.8 GPa which is much higher than the modulus values measured by DMA for similar exposure times. Indeed, for t varying from 10 min to 20 min, when analyzing the samples in DMA at 20 °C and at a frequency of 1 Hz, it comes: 3.8 MPa $\leq E \leq$ 56 MPa (Table 2). However, in AFM nanoindentation, our experimental set-up operates at a much higher frequency: f_{AFM} = 2 kHz. If we refer to the master curves of the sample presented in Figure 11B, the mechanical response of the material is very close to the glassy plateau at this frequency. It is thus expected that the measured moduli will be much higher than those measured at 1 Hz (*e.g.* in the GPa range). In

these conditions, AFM nanoindentation is not adapted to probe small variations of modulus. However, it is still useful to reveal large gradients such as the one existing between the samples crosslinked for 10 min *versus* 240 min (for z = 100 μm, Figure 12A). On this basis, we decided to record the modulus at a very different depth, for long exposure times. Figure 12B represents the moduli measured at z = 1.4 mm, for t = 120 min and t = 240 min (The corresponding Young's modulus mapping are reported Figures S23 and S24). These moduli are slightly inferior to those measured at z = 100 μm for similar exposure times, but above those measured for t = 10 min and 20 min. They indicate the existence of a depth gradient of moderated amplitude. This last result is well consistent with the observations made in Raman spectroscopy, which indicated that photo-crosslinking reaction still proceeds relatively well beyond 1 mm beneath the surface, for exposure times > 2h. It confirms the good homogeneity of the samples from both the chemical and the mechanical viewpoints.

Conclusion

To conclude, a UV-curable cinnamate-functionalized polybutadiene was synthesized *via* an efficient thiol-ene approach. The resulting polymer was used to conceive millimeter thick object with a photo-tunable elastic modulus, that can be adjusted over 2 orders of magnitude, from a few MPa to more than 1 GPa. The good efficiency of the photo-crosslinking reaction was confirmed with numerous experimental approaches including photo-rheology, FTIR and Raman spectroscopies, and gel content analysis. Because a gradient of elastic modulus was anticipated across the millimeters-thick samples, they were further analyzed by performing depth-profiling of both the crosslink density and the mechanical properties. Raman spectroscopy was employed to investigate the conversion of the photo-dimerization reaction along the cross-section of the cut samples. Additionally, AFM nanoindentation was used to measure the local elastic modulus at varying distances from the irradiated surface. The results revealed depth gradients, particularly for shorter exposure times (*e.g.*, 5 min ≤ t ≤ 20 min). For longer exposure durations (*e.g.*, t ≥ 120 min), the samples appeared largely homogeneous. This unprecedented investigation of the photo-dimerization yield and the mechanical properties, in both time and space, for a UV-curable rubber, offers valuable insights for applications requiring soft materials with photo-tunable mechanical properties. It is of particular interest when these materials are used as propagating medium of elastic waves for instance. Soft metamaterials (*e.g.* frequency filters, acoustic lenses) are among the list of relevant examples.[62, 63]

Finally, it must be emphasized that the reversed reaction, *i.e.* the decrosslinking of the materials, remains unachievable with these types of UV-curable systems. Indeed, the cleavage of the cinnamate dimers is triggered by ~ 250 nm wavelengths, *i.e.* deep UV. Thus, the energy of the corresponding photons, that is inversely proportional to the wavelength, is high. This limits the penetration depth within the material, while increasing the risk of degradation due to the strong interaction with the polymer. As expected, all the decrosslinking attempts were either ineffective or resulted in severe degradation of the material. Although newly discovered photo-dimerizable moieties can be reversibly associated and dissociated at longer wavelengths,[21] such as pyrene–chalcone[64] or styrylquinoxaline,[65] they have not yet been utilized in the development of materials with reversible mechanical properties. These new chemistries still have to be implemented in elastomeric systems, and further investigation into the efficiency of the photo-crosslinking reaction within the bulk of the materials will be necessary, as proposed in this study. They will help in the preparation of the next generation of adaptable and reusable materials, *via* photo-mediated processes.

Associated Content

ESI: Characterization of the thio-cinnamate ester, Additional NMR and FTIR characterizations of **TC-PBut**, SEC analyses of **TC-PBut**, TGA analyses of **TC-PBut**, DSC analyses of **TC-PBut** and photo-crosslinked samples, Additional DMA analyses of photo-crosslinked samples.

Note

The authors declare no competing financial interest.

Acknowledgements

This study received financial support from the French government in the framework of the University of Bordeaux's IdEx "Investments for the Future" program/ GPR PPM. SC is grateful to the University of Bordeaux for the funding of an interdisciplinary Ph.D. grant.

References

(1) Roh, Y.; Lim, D.; Kang, M.; Cho, J.; Han, S.; Ko, S. H. Rigidity-Tunable Materials for Soft Engineering Systems. *Advanced Engineering Materials* **2024**, *26* (13). DOI: 10.1002/adem.202400563.

(2) Cheng, N. G.; Gopinath, A.; Wang, L.; Iagnemma, K.; Hosoi, A. E. Thermally Tunable, Self-Healing Composites for Soft Robotic Applications. *Macromolecular Materials and Engineering* **2014**, *299* (11), 1279-1284. DOI: 10.1002/mame.201400017.

(3) Ji, S.; Wu, X.; Jiang, Y.; Wang, T.; Liu, Z.; Cao, C.; Ji, B.; Chi, L.; Li, D.; Chen, X. Self-Reporting Joule Heating Modulated Stiffness of Polymeric Nanocomposites for Shape Reconfiguration. *Acs Nano* **2022**, *16* (10), 16833-16842. DOI: 10.1021/acsnano.2c06682.

(4) Cao, Z.; Clark, A. T.; Vite, A.; Corbin, E. A. A Dynamic Gradient Stiffness Material Platform to Manipulate Cardiac Fibroblasts' Spatio-Temporal Behavior. *Advanced Functional Materials* **2024**, ; Early Access. DOI: 10.1002/adfm.202402808.

(5) Gliozzi, A. S.; Miniaci, M.; Chiappone, A.; Bergamini, A.; Morin, B.; Descrovi, E. Tunable photo-responsive elastic metamaterials. *Nature Communications* **2020**, *11* (1). DOI: 10.1038/s41467-020-16272-y.

(6) Hiemenz, P. C.; Lodge, T. P. *Polymer Chemistry*; CRC Press, 2007. DOI: 10.1201/9781420018271.

(7) Brighenti, R.; Cosma, M. P. Smart actuation of liquid crystal elastomer elements: cross-link density-controlled response. *Smart Materials and Structures* **2022**, *31* (1). DOI: 10.1088/1361-665X/ac34bf.

(8) Streicher, M.; Stamp, C.-H.; Kluth, M. D.; Ripp, A.; Calvino, C. Harnessing the Photoperformance of *N*-Methyl-Quinolinone for Gated Photo-Driven Cyclability and Reversible Photoligation. *Macromolecular Rapid Communications* **2024**, ; Early Access. DOI: 10.1002/marc.202400474.

(9) Zhang, R.; Lai, M.; Bai, H.; Ma, H.; Han, L. Stimuli responsive dynamic polymer networks with tunable toughness and elasticity through the regulation of covalent crosslinking and reversible hydrogen bonds. *Journal of Materials Chemistry C* **2024**, *12* (23), 8525-8533. DOI: 10.1039/d4tc01309c.

(10) Li, J.; Lewis, C. L.; Chen, D. L.; Anthamatten, M. Dynamic Mechanical Behavior of Photo-Cross-linked Shape-Memory Elastomers. *Macromolecules* **2011**, *44* (13), 5336-5343. DOI: 10.1021/ma2004019.

(11) Sugimoto, K.; Hayashi, M.; Kawarazaki, I.; Ito, S. Versatile tensile and fracture behaviors of dual cross-linked elastomers by postpreparation photo tuning of local cross-link density. *Polymer* **2021**, *230*. DOI: 10.1016/j.polymer.2021.124089.

(12) Accardo, J. V.; Kalow, J. A. Reversibly tuning hydrogel stiffness through photocontrolled dynamic covalent crosslinks. *Chemical Science* **2018**, *9* (27), 5987-5993. DOI: 10.1039/c8sc02093k.

(13) Kabb, C. P.; O'Bryan, C. S.; Deng, C. C.; Angelini, T. E.; Sumerlin, B. S. Photoreversible Covalent Hydrogels for Soft-Matter Additive Manufacturing. *Acs Applied Materials & Interfaces* **2018**, *10* (19), 16793-16801. DOI: 10.1021/acsami.8b02441.

(14) Duval, A.; Averous, L. From thermoplastic polyurethane to covalent adaptable network *via* reversible photo-crosslinking of a biobased chain extender synthesized from caffeic acid. *Polymer Chemistry* **2023**, *14* (22), 2685-2696. DOI: 10.1039/d3py00162h.

(15) Yan, R.; Jin, B.; Luo, Y.; Li, X. Optically healable polyurethanes with tunable mechanical properties. *Polymer Chemistry* **2019**, *10* (18), 2247-2255. DOI: 10.1039/c9py00261h.

(16) Tamate, R.; Ueki, T.; Kitazawa, Y.; Kuzunuki, M.; Watanabe, M.; Akimoto, A. M.; Yoshida, R. Photo-Dimerization Induced Dynamic Viscoelastic Changes in ABA Triblock Copolymer-Based Hydrogels for 3D Cell Culture. *Chemistry of Materials* **2016**, *28* (17), 6401-6408. DOI: 10.1021/acs.chemmater.6b02839.

(17) Aljuaid, M.; Chang, Y.; Haddleton, D. M.; Wilson, P.; Houck, H. A. Thermoreversible 2+2 Photodimers of Monothiomaleimides and Intrinsically Recyclable Covalent Networks Thereof. *Journal of the American Chemical Society* **2024**, *146* (28), 19177-19182. DOI: 10.1021/jacs.4c04193.

(18) Masai, H.; Nakagawa, T.; Terao, J. Recent progress in photoreactive crosslinkers in polymer network materials toward advanced photocontrollability. *Polymer Journal* **2024**, *56* (4), 297-307, Review. DOI: 10.1038/s41428-023-00875-5.

(19) Kaur, G.; Johnston, P.; Saito, K. Photo-reversible dimerisation reactions and their applications in polymeric systems. *Polymer Chemistry* **2014**, *5* (7), 2171-2186, Review. DOI: 10.1039/c3py01234d.

(20) Calvino, C. Photocycloadditions for the Design of Reversible Photopolymerizations. *Chimia* **2022**, *76* (10), 816-825. DOI: 10.2533/chimia.2022.816.

(21) Truong, V. X.; Barner-Kowollik, C. Photodynamic covalent bonds regulated by visible light for soft matter materials. *Trends in Chemistry* **2022**, *4* (4), 291-304, Review. DOI: 10.1016/j.trechm.2022.01.011.

(22) Frisch, H.; Marschner, D. E.; Goldmann, A. S.; Barner-Kowollik, C. Wavelength-Gated Dynamic Covalent Chemistry. *Angewandte Chemie-International Edition* **2018**, *57* (8), 2036-2045, Review. DOI: 10.1002/anie.201709991.

(23) Blasco, E.; Wegener, M.; Barner-Kowollik, C. Photochemically Driven Polymeric Network Formation: Synthesis and Applications. *Advanced Materials* **2017**, *29* (15), Review. DOI: 10.1002/adma.201604005.

(24) Tunc, D.; Le Coz, C.; Alexandre, M.; Desbois, P.; Lecomte, P.; Carlotti, S. Reversible Cross-Linking of Aliphatic Polyamides Bearing Thermo- and Photoresponsive Cinnamoyl Moieties. *Macromolecules* **2014**, *47* (23), 8247-8254. DOI: 10.1021/ma502083p.

(25) Durand, P. L.; Brege, A.; Chollet, G.; Grau, E.; Cramail, H. Simple and Efficient Approach toward Photosensitive Biobased Aliphatic Polycarbonate Materials. *Acs Macro Letters* **2018**, *7* (2), 250-254. DOI: 10.1021/acsmacrolett.8b00003.

(26) Defize, T.; Thomassin, J.-M.; Ottevaere, H.; Malherbe, C.; Eppe, G.; Jellali, R.; Alexandre, M.; Jerome, C.; Riva, R. Photo-Cross-Linkable Coumarin-Based Poly(ε-caprolactone) for Light-Controlled Design and Reconfiguration of Shape-Memory Polymer Networks. *Macromolecules* **2019**, *52* (2), 444-456. DOI: 10.1021/acs.macromol.8b02188.

(27) Chen, Y.; Geh, J. L. Copolymers derived from 7-acryloyloxy-4-methylcoumarin and acrylates .1. Copolymerizability and photocrosslinking behaviours. *Polymer* **1996**, *37* (20), 4473-4480. DOI: 10.1016/0032-3861(96)00299-6.

(28) Trakhtenberg, S.; Warner, J. C.; Nagarajan, R.; Bruno, F. F.; Samuelson, L. A.; Kumar, J. Spectroscopic and microscopic analysis of photo-cross-linked vinylbenzylthymine copolymers

for photoresist applications. *Chemistry of Materials* **2006**, *18* (12), 2873-2878. DOI: 10.1021/cm0515303.

(29) Almutairi, F.; Monier, M.; Alatawi, R.; Alhawiti, A.; Al-Rasheed, H.; Almutairi, T.; Elsayed, N. Synthesis of photo-crosslinkable hydrogel membranes for entrapment of lactase enzyme. *Reactive & Functional Polymers* **2022**, *172*. DOI: 10.1016/j.reactfunctpolym.2022.105159.

(30) Frateur, O.; Becelaere, J.; Merckx, R.; Van Guyse, J.; Purino, M.; Hoogenboom, R.; De Clerck, K. Development of reversibly photo-crosslinkable water-stable poly (2-ethyl-2-oxazoline) nanofibers via functionalization with cinnamoyl moieties. *European Polymer Journal* **2024**, *212*. DOI: 10.1016/j.eurpolymj.2024.113076.

(31) Hoskins, J. A. The Occurrence, Metabolism and Toxicity of Cinnamic Acid and Related-Compounds. *Journal of Applied Toxicology* **1984**, *4* (6), 283-292, Review. DOI: 10.1002/jat.2550040602.

(32) Kanokwijitsilp, T.; Koerner, M.; Prucker, O.; Anton, A.; Luebke, J.; Ruehe, J. Kinetics of Photocrosslinking and Surface Attachment of Thick Polymer Films. *Macromolecules* **2021**, *54* (13), 6238-6246. DOI: 10.1021/acs.macromol.1c00121.

(33) Koo, G.-H.; Jang, J. Depth-gradient and photoinitiator-free photocrosslinking of poly(ethylene oxide). *Journal of Applied Polymer Science* **2012**, *125* (4), 2659-2667. DOI: 10.1002/app.36438.

(34) Lim, K. S.; Klotz, B. J.; Lindberg, G. C. J.; Melchels, F. P. W.; Hooper, G. J.; Malda, J.; Gawlitta, D.; Woodfield, T. B. F. Visible Light Cross-Linking of Gelatin Hydrogels Offers an Enhanced Cell Microenvironment with Improved Light Penetration Depth. *Macromolecular Bioscience* **2019**, *19* (6). DOI: 10.1002/mabi.201900098.

(35) Wu, W.; Karamdoust, S.; Turowec, B. A.; Gillies, E. R. Synthesis and application of cinnamate-functionalized rubber for the preparation of UV-curable films. *European Polymer Journal* **2013**, *49* (12), 4238-4248. DOI: 10.1016/j.eurpolymj.2013.10.003.

(36) Visconte, L. L. Y.; Andrade, C. T.; Azuma, C. UV-light induced crosslinking reaction of cinnamate natural rubbers: Effect of the spacer length, counter-ion nature, and content. *Journal of Applied Polymer Science* **1998**, *69* (5), 907-910. DOI: 10.1002/(sici)1097-4628(19980801)69:5<907::aid-app9>3.0.co;2-q.

(37) Visconte, L. L. Y.; Andrade, C. T.; Azuma, C. Photosensitivity of Modified Natural Polyisoprenes as Function of the Alipathic Side-Chain. *Polymer Bulletin* **1991**, *25* (2), 217-223. DOI: 10.1007/bf00310795.

(38) Visconte, L. L. Y.; Andrade, C. T.; Azuma, C. Kinetic Treatment for the Photodimerization Reaction of Modified Natural Polyisoprenes. *Polymer Bulletin* **1991**, *26* (6), 637-641. DOI: 10.1007/bf00313218.

(39) Derouet, D.; Phinyocheep, P.; Boccaccio, G.; Brosse, J. Synthesis of photo-crosslinkable elastomers by chemical modification of liquid natural rubber. *J. Nat. Rubb. Res* **1991**, *6*, 39-54.

(40) Azuma, C.; Sanui, K.; Ogata, N. Synthesis and Properties of Photosensitive Rubbers .2. Photosensitivity of Cyclized Polydienes and Polypentenamer with Pendent Cinnamate Groups. *Journal of Applied Polymer Science* **1982**, *27* (6), 2065-2078.

(41) Derjaguin, B.; Muller, V.; Toporov, Y. Effect Of Contact Deformations on Adhesion of Particles. *Journal of Colloid and Interface Science* **1975**, *53*, 314-326.

(42) David, R. L. A.; Kornfield, J. A. Facile, efficient routes to diverse protected thiols and to their deprotection and addition to create functional polymers by thiol-ene coupling. *Macromolecules* **2008**, *41* (4), 1151-1161. DOI: 10.1021/ma0718393.

(43) Justynska, J.; Hordyjewicz, Z.; Schlaad, H. Toward a toolbox of functional block copolymers via free-radical addition of mercaptans. *Polymer* **2005**, *46* (26), 12057-12064. DOI: 10.1016/j.polymer.2005.10.104.

(44) Kraus, G.; Moczvgem G. A. Chain Entanglements and Elastic Behavior of Polybutadiene Networks. *Journal of Polymer Science Part A-General Papers* **1964**, *2*, 277-288.

(45) Lowe, A. Thiol-ene "click" reactions and recent applications in polymer and materials synthesis: a first update. *Polymer Chemistry* **2014**, *5* (17), 4820-4870. DOI: 10.1039/c4py00339j.

(46) Chesterman, J.; Hughes, T.; Amsden, B. Reversibly photo-crosslinkable aliphatic polycarbonates functionalized with coumarin. *European Polymer Journal* **2018**, *105*, 186-193. DOI: 10.1016/j.eurpolymj.2018.05.038.

(47) Wang, Z.; Randazzo, K.; Hou, X.; Simpson, J.; Struppe, J.; Ugrinov, A.; Kastern, B.; Wysocki, E.; Chu, Q. Stereoregular Two-Dimensional Polymers Constructed by Topochemical Polymerization. *Macromolecules* **2015**, *48*, 2894-2900. DOI: 10.1021/acs.macromol.5b00109.

(48) Sung, S.; Cho, K.; Hah, H.; Lee, J.; Shim, H.; Park, J. Two different reaction mechanisms of cinnamate side groups attached to the various polymer backbones. *Polymer* **2006**, *47*, 2314-2321. DOI: 10.1016/j.polymer.2006.02.003.

(49) Barbet, F.; Bormann, D.; Warenghem, M.; Khelifa, B.; Kurios, Y.; Reznikov, Y.; Simoni, F. Comparative Raman spectroscopy studies of photosensitive polymers. *Materials Chemistry And Physics* **1998**, *55*, 202-208.

(50) Fox, T.; Loshaek, S. Influence of Molecular Weight and Degree of Crosslinking on the Specific Volume and Glass Temperature of Polymers. *Journal Of Polymer Science* **1955**, *15*, 371-390.

(51) Flory, P. J.; Rehner, J. Statistical mechanics of cross-linked polymer networks II Swelling. *Journal of Chemical Physics* **1943**, *11* (11), 521-526. DOI: 10.1063/1.1723792.

(52) Rubinstein, M.; Colby, R. H. *Polymer physics*; Oxford university press, 2003.

(53) Ferry, J. D. *Viscoelastic Properties of Polymers*; Wiley, 1980.

(54) Mailhot, N.; Morlat-Thérias, S.; Bussière, P.; Gardette, J. Study of the degradation of an epoxy/amine resin, 2 kinetics and depth-profiles. *Macromolecular Chemistry And Physics* **2005**, *206*, 585-591. DOI: 10.1002/macp.200400394.

(55) Mailhot, B.; Bussière, P.; Rivaton, A.; Morlat-Thérias, S.; Gardette, J. Depth profiling by AFM nanoindentations and micro-FTIR spectroscopy for the study of polymer ageing. *Macromolecular Rapid Communications* **2004**, *25*, 436-440. DOI: 10.1002/marc.200300110.

(56) Gu, X.; Michaels, C. A.; Drzal, P. L.; Jastnin, J.; Martin, D.; Nguyen, T.; Martin, J. W. Probing photodegradation beneath the surface: a depth profiling study of UV-degraded polymeric coatings with microchemical imaging and nanoindentation. *Journal of Coatings Technology and Research* **2007**, *4* (4), 389-399, ; Proceedings Paper. DOI: 10.1007/s11998-007-9052-x.

(57) Zhang, S.; Weng, Y.; Ma, C. Quantitative Nanomechanical Mapping of Polyolefin Elastomer at Nanoscale with Atomic Force Microscopy. *Nanoscale Research Letters* **2021**, *16*. DOI: 10.1186/s11671-021-03568-1.

(58) Young, T.; Monclus, M.; Burnett, T.; Broughton, W.; Ogin, S.; Smith, P. The use of the PeakForce™ quantitative nanomechanical mapping AFM-based method for high-resolution Young's modulus measurement of polymers. *Measurement Science and Technology* **2011**, *22*. DOI: 10.1088/0957-0233/22/12/125703.

(59) Cappella, B. *Mechanical Properties of Polymers Measured through AFM Force-Distance Curves*; Springer, 2016.

(60) VanLandingham, M.; Chang, N.; Drzal, P.; White, C.; Chang, S. Viscoelastic characterization of polymers using instrumented indentation. I. Quasi-static testing. *Journal of Polymer Science Part B-Polymer Physics* **2005**, *43*, 1794-1811. DOI: 10.1002/polb.20454.

(61) White, C.; Vanlandingham, M.; Drzal, P.; Chang, N.; Chang, S. Viscoelastic characterization of polymers using instrumented indentation. II. Dynamic testing. *Journal of Polymer Science Part B-Polymer Physics* **2005**, *43*, 1812-1824. DOI: 10.1002/polb.20455.

(62) Jin, Y.; Kumar, R.; Poncelet, O.; Mondain-Monval, O.; Brunet, T. Flat acoustics with soft gradient-index metasurfaces. *Nature Communications* **2019**, *10*. DOI: 10.1038/s41467-018-07990-5.

(63) Lombard, O.; Kumar, R.; Mondain-Monval, O.; Brunet, T.; Poncelet, O. Quasi-flat high-index acoustic lens for 3D underwater ultrasound focusing. *Applied Physics Letters* **2022**, *120*. DOI: 10.1063/5.0088503.

(64) Irshadeen, I.; De Bruycker, K.; Micallef, A.; Walden, S.; Frisch, H.; Barner-Kowollik, C. Green light LED activated ligation of a scalable, versatile chalcone chromophore. *Polymer Chemistry* **2021**, *12* (34), 4903-4909. DOI: 10.1039/d1py00533b.

(65) Kalayci, K.; Frisch, H.; Truong, V.; Barner-Kowollik, C. Green light triggered [2+2] cycloaddition of halochromic styrylquinoxaline-controlling photoreactivity by pH. *Nature Communications* **2020**, *11* (1). DOI: 10.1038/s41467-020-18057-9.